Zamudio-Ramirez, I.; Saucedo-Dorantes, JJ.; Antonino-Daviu, JA.; Osornio-Rios, RA.; Dunai, L. (2022). Detection of Uniform Gearbox Wear in Induction Motors based on the Analysis of Stray Flux Signals through Statistical Time-Domain Features and Dimensionality Reduction Techniques. IEEE Transactions on Industry Applications. 58(4):4648-4656. https://doi.org/10.1109/TIA.2022.3174049

Detection of Uniform Gearbox Wear in Induction Motors based on the Analysis of Stray Flux Signals through Statistical Time-Domain Features and Dimensionality Reduction Techniques

I. Zamudio-Ramirez, J. J. Saucedo-Dorantes, *IEEE Member*, J. A. Antonino-Daviu, *IEEE Senior Member*, R. A. Osornio-Rios, *IEEE Senior Member*, and L. Dunai, *IEEE Member*

***Abstract*—Gearboxes are core elements in power transmission systems, although gearboxes are reliable and high-efficiency components, the occurrence of different faults is frequent since they are often subjected to adverse operating conditions. Classical gearbox condition monitoring approaches are based on the analysis of vibration and current motor signals and rely on the identification of specific fault-related frequency patterns. In this regard, this paper proposes a novel diagnosis methodology based on the analysis of stray flux signals for detecting uniform wear in the gear teeth. The proposed methodology is based on the processing of the stray flux signals through feature calculation and extraction stages that lead to a high-performance signal characterization by estimating a set of statistical time domain-based features and then reducing the dimensionally by means of the PCA and LDA techniques. Additionally, an automatic fault diagnosis is achieved through a Neural Network-based classifier for the detection and identification of uniform wear in a gearbox. The obtained results prove the potential of the proposal for its incorporation in condition maintenance programs in the industry, becoming an excellent alternative to classical approaches.**

***Index Terms*— Gearbox wear, fault diagnosis, induction motor, stray flux, feature extraction, Linear discriminant analysis.**

I. INTRODUCTION

THE implementation of Condition-based maintenance (CMB) programs has played a key role in industrial sites to ensure the proper working condition and availability of industrial machinery [1]. Indeed, most of the industrial applications are based on electromechanical systems or kinematic chains where multiple electromechanical configurations can be made by involving the use of Induction Motors (IM), couplings, shafts, belts, pulleys, and gearboxes. Generally, most of these elements are mechanically coupled to be part of Power Transmission Systems (PTS) that may be found in many industrial applications in aerospace, heavy-duty industry, wind turbines, and machining tools [2], [3]. Certainly, although gearboxes are the key element of PTS due to their high efficiency and robustness [3], adverse operating conditions produce constant stresses causing gradual wear on the gear teeth that can lead to an unacceptable reduction of their performance [4]. In this sense, the development of effective and reliable condition monitoring strategies for the assessment and detection of incipient faults such as the uniform wear in gearboxes is necessary.

A great deal of condition monitoring strategies based on the analysis of vibration, stator currents, torque, and sound have been proposed to diagnose discrete faults in gearboxes like broken or chipped teeth [1], [2], [4]. In this regard, it has been proved that the fault identification in gearboxes can be associated to the amplitude increase of the characteristic fault-related frequency components and sidebands in a vibration spectrum [1], [5]; whereas, the fault detection may be also performed by analyzing the modulation effects on stator current spectrum [6], by using the bispectrum analysis [7], and/or by applying time-frequency decomposition (*TFD*) methods [8]. Despite vibrations and stator currents have classically used to to assess the gearbox condition, the analysis of torque and sound signals in the time-frequency domain, i.e. Wavelet transform, have led to the detection of gearbox faults [9]-[10].

Regarding the use of stray flux signals to diagnose gearbox faults, only few works can be found in the available literature [11]-[12]. However, the analysis of stray flux signals can help to achieve accurate diagnosis in comparison with classical analyses that are based on vibrations or stator currents, since the rotor magneto-motive forces (MMF) or stray fluxes are less influenced by oscillations in the load compared to other quantities [13]-[16]. Accordingly, based on the results obtained by [11] and [12], the analysis of stray flux signals in the steady-state allows the detection of gearbox faults due to the amplitude increase of specific fault-related patterns. Yet, although gearbox faults may be detected by the analysis of stray flux signals, some limitations that affect the diagnosis must be faced, i.e., the sensitivity of signal-to-noise ratio, inadequacy for nonstationary signals, spectral leakage, and loss of information related to time. Thus, it is mandatory to propose new alternatives based on stray flux signals that can overcome all these drawbacks.

On the other hand, the development of intelligent condition monitoring strategies able to achieve the automatic fault

This work was partially supported by supported by the Spanish 'Ministerio de Ciencia Innovación y Universidades' and FEDER program in the 'Proyectos de I+D de Generación de Conocimiento del Programa Estatal de Generación de Conocimiento y Fortalecimiento Científico y Tecnológico del Sistema de I+D+i, Subprograma Estatal de Generación de Conocimiento' (ref: PGC2018-095747-B-I00), and by the Consejo Nacional de Ciencia y Tecnología (CONACyT) under scholarship 652815. *Corresponding author: J. A. Antonino-Daviu (e-mail: joanda@die.upv.es).* The authors contributed equally.

J. J. Saucedo-Dorantes and R. A. Osornio-Rios are with HSPdigital CA-Mecatronica Engineering Faculty, Autonomous University of Queretaro, San Juan del Rio 76806, Mexico. (e-mail: jsaucedo@hspdigital.org, rao-sornio@hspdigital.org).

I. Zamudio-Ramirez, and J. A. Antonino-Daviu are with the Instituto Tecnológico de la Energía, Universitat Politècnica de València (UPV), Camino de Vera s/n, 46022 Valencia, Spain. (e-mail: iszara@doctor.upv.es, joanda@die.upv.es)

L. Dunai is with the Centro de Investigación en Tecnologías Gráficas, Universitat Politècnica de València, Camino de Vera s/n, 46022, Valencia, SPAIN (e-mail: ladu@upv.es).

diagnosis may improve the condition assessment of those analyses that are dependent on the user expertise, i.e., the amplitude increase of the characteristic fault-related patterns in a frequency spectrum. In this context, feature calculation and feature reduction stages in condition monitoring approaches are considered to achieve a high-performance characterization of the fault-related patterns. Thus, the feature calculation aims to obtain a meaningful pool of features that are estimated through the analysis of the acquired raw signals in different domains such as time domain (*TD*), frequency domain (*FD*) and time-frequency domain (*TFD*); i.e., by estimating a set of statistical features from *TD* analysis [17]. While, the feature reduction is performed to extract the most significative information from an original pool of features that is commonly represented into a high-dimensional space; i.e., the original pool of features is subjected to a reduction procedure by means of the Principal Component Analysis (PCA) and the Linear Discriminant Analysis (LDA). Finally, the automatic fault detection may be achieved by considering artificial intelligence algorithms such as Artificial Neural-Networks (ANN), Support Vector Machines (SVM), Fuzzy classifiers, among others. In fact, condition monitoring strategies that incorporate the feature calculation and feature reduction, even classification algorithms are capable of detecting the occurrence of a fault in rotating electrical or mechanical machines [17]-[18].

This work is based on the proposal of a novel non-invasive diagnosis methodology capable of detecting different levels of uniform wear on the gear teeth of a gearbox, the gearbox wear detection is performed by analyzing stray flux signals that are acquired through different sensors installed in the frame of the IM that drives the gearbox under study. The gearbox wear assessment is achieved by characterizing the acquired signals through the estimation of a significant set of 15 statistical time-domain features to obtain the fault-related patterns that characterize the fault occurrence. Subsequently, the estimated set of statistical features is subjected to a dimensionality reduction process by means of the PCA and the LDA aiming to analyze the data distribution and to obtain a 2-D representation of the evaluated conditions. Then, through a Neural Network-based classifier, the automatic diagnosis of four different conditions (healthy condition and three different levels of uniform wear on the gear teeth, 25%, 50% and 75%) is performed. Finally, an analysis and validation of the acquired signals is also performed by means of the short-time MUSIC algorithm reported in [19]. Such analysis is included to identify the effects that the occurrence of uniform wear on the gear teeth induces over the stray flux signals. The obtained results demonstrate the effectiveness of the proposed diagnosis methodology for being included as a part of the condition-based maintenance programs in industrial applications, becoming an excellent alternative versus classical approaches.

II. Theoretical Background

In this section are presented the theoretical basis that must be considered to perform the proposed condition monitoring strategy, where, the aim of including dimensionality reduction techniques such as Principal Component Analysis (PCA) and the Linear Discriminant Analysis (LDA) is the analysis of the data distribution and the reduction of an original feature space; as well as, the description of the most important aspects considered in the Neural Network (NN) that is used to achieve the automatic fault diagnosis and classification of faults.

A. Dimensionality reduction

Feature calculation and dimensionality reduction techniques play an important role when they are part of condition monitoring strategies. Feature calculation refers to the signal processing methods that have the goal of obtaining the specific patterns that characterize that signal [20]; on the other hand, dimensionality reduction techniques may be used for different purposes, e.g., the analysis of data distributions and/or the reduction of an original feature space that may not be visually represented. In this regard, the Principal Component Analysis (PCA) and the Linear Discriminant Analysis (LDA) are two well-known dimensionality reduction techniques in the field of machine learning [17].

Both PCA and LDA can be used as a way of reducing the dimensionality of the data set, but PCA is an unsupervised technique while LDA is supervised. Thus, both techniques have different goals, PCA aims to map an original data set into the coordinate axis that is most convenient for representing the data set, retaining as much as possible the data variance. The data mapped by the PCA do not consider any classification information and this technique is more convenient to represent an original data set into reduced dimensionality representation with the minimization of information loss. On the other hand, since LDA considers classification information, it aims to map the original data set into another coordinate axis in which the maximum linear separation between different classes is intended; thus, multi-class problems represented by complex and high-dimensional data sets become easier to be distinguished through the LDA. This is possible since all considered classes can be distinguished and represented into a low dimensional feature space, while reducing the large amount of computations required [18].

B. Neural Network-based classifiers

Certain algorithms and methods used in computational learning allow to obtain the prediction of events once a specific model has been trained with known data, in addition, after the training procedure it is desired to obtain precise answers, if not identical, the most similar to the correct one. In this regard, from the viewpoint of condition monitoring and automatic diagnosis, the Neural Network-based classifiers have been widely used in several applications where the detection of unexpected conditions is the goal to be achieved. Several configurations may be considered when using NN's, however, the basic structure comprises three main layers, the input, hidden, and output layers that must be defined with a specific number of neurons [21]. Therefore, for condition monitoring approaches, the input layer has as many neurons as many as characteristic features are available; in the hidden layer can be defined a number of neurons equivalent to three, four, or five times the

number of neurons of the hidden layer; and, in the output layer are defined as many neurons as many conditions are evaluated [22].

III. PROPOSED METHODOLOGY

The flowchart shown in Fig. 1 depicts the proposed diagnosis methodology which is mainly based on five steps. First, the different fault conditions are experimentally developed in a kinematic chain, namely: the healthy condition and three different levels of uniform wear on the gear teeth (25%, 50% and 75% of uniform wear) are evaluated. The second step relies on the data acquisition, where, the stray flux signals generated in the IM during its operation are continuously acquired by means of the data acquisition system (DAS) module proposed in [23]. The stray flux signals are continuously measured by means of proprietary Hall-effect tri-axial sensors allowing the acquisition of the radial stray flux (ϕ_1), axial stray flux (ϕ_2), and axial + radial stray flux (ϕ_3).

Subsequently, in the third step of feature calculation, each acquired signal is characterized by means of estimating a meaningful set of statistical time domain-based features; hence, a set of 15 statistical features is estimated and composed by: the mean, maximum value, RMS, square root mean, standard deviation, variance, RMS shape factor, square root mean shape factor, crest factor, latitude factor, impulse factor, skewness, kurtosis, and normalized fifth and sixth moments. As a result, a characteristic feature matrix with $TD = 45$ statistical features is computed, $\mathbf{T} \in \mathbb{R}^{TD}$. In fact, it has been proven that this set of features allows achieving a high-performance signal characterization due to its capability for modeling trends and changes in signals. The corresponding mathematical equations of these features may be found in [17].

After that, in the fourth step is performed the feature reduction, where, two well-known feature reduction techniques are employed, PCA and LDA. Thereby, the PCA is first used to analyze the variability of the data distribution of characteristic feature matrix $\mathbf{T} \in \mathbb{R}^{T}$ that represents the evaluated conditions. Thus, given a data matrix $\mathbf{T}$ with $M = TD$ columns representing features and N rows representing samples, the PCA is performed as follows:

The estimation of the covariance matrix by (1):

$$\boldsymbol{C} = \frac{\sum_{n=1}^{N}(T_n - \bar{T})\,(T_n - \bar{T})'}{N-1} \tag{1}$$

where, $\boldsymbol{C}$ is the covariance matrix, T_n the n-th vector and $\bar{T}$ the mean of the n-th vector of the feature matrix $\mathbf{T} \in \mathbb{R}^{T}$. Then, the eigenvalues and eigenvector of $\boldsymbol{C}$ are computed by (2):

$$\boldsymbol{C} = \sum_{m=1}^{M} \lambda_m v_m v_m' = V \Lambda V' \tag{2}$$

where v_m and λ_m are the mth eigenvector and eigenvalue of $\boldsymbol{C}$, respectively, and V and Λ represent the corresponding eigenvectors and eigenvalues of $\boldsymbol{C}$, respectively. And Finally, the eigenvalues are sorted from largest to smallest and the individual and cumulative contribution rates of the considered feature are estimated by (3) and (4), respectively:

$$p\iota = \lambda\iota \Big/ \sum_{\iota=1}^{M} \lambda\iota \tag{3}$$

$$\bar{p} = \sum_{\iota=1}^{M} p\iota \tag{4}$$

wehere, $p\iota$ is is the contribution rate of the Ith component, $\lambda\iota$ is the Ith eigenvalue arranged from large to small and $\bar{p}$ represents the cumulative contribution rate. In this regard, the individual and cumulative contribution rates estimated by (3) and (4) depicts the variability of the data distribution and are considered to identify the minimum space into which the original feature space (45-D) may be represented by retaining as much as possible its variance, which is desired to be the 2-D or 3-D space.

Subsequently, as a part of the same feature reduction step, the LDA technique is applied over the feature matrix $\mathbf{T} \in \mathbb{R}^{T}$ aiming to reduce the original feature space (45-D) by means of a linear transformation that attempts to maximize as much as possible the linear distance between considered conditions; that is carried out as described below:

The LDA is based of the solution of a multi-class problem, thus, for Q-classes is supported by the estimation of the the between-class scatter matrix ($\boldsymbol{S_b}$) and the within-class scatter matrix ($\boldsymbol{S_w}$) following (5) and (6), respectively:

$$\boldsymbol{S_b} = \sum_{j=1}^{Q} N_j (m_j - \bar{m})(m_j - \bar{m})^T \tag{5}$$

$$\boldsymbol{S_w} = \sum_{j=1}^{Q} \sum_{i=1}^{N_j} (x_i^j - m_j)(x_i^j - m_j)^T = \sum_{j=1}^{Q} S_{w_j} \tag{6}$$

where, N_j represents the total number of samples for the j-th class Q_j, $\bar{m}$ represents the mean of all the samples, m_j the mean of the class Q_j, x_i^j the ith sample of the class Q_j. The objective of the LDA is to find an optimal projection matrix $\boldsymbol{W}$ where the ratio between matrices $\boldsymbol{S_b}$ and $\boldsymbol{S_w}$ is maximized, such

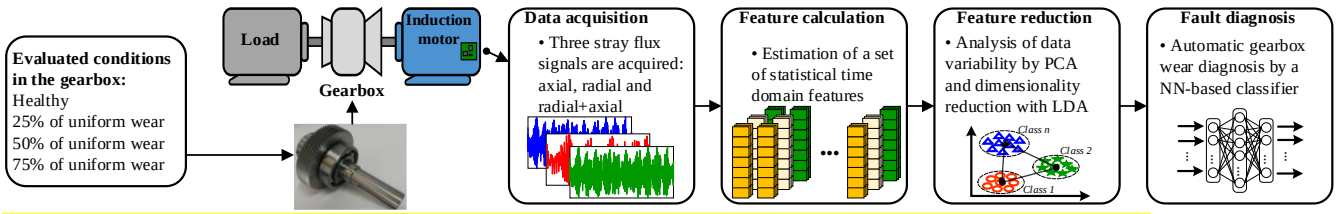

Fig. 1. Proposed diagnosis methodology based on the analysis of stray flux signals for the diagnosis of uniform wear on the gear teeth.

maximization is performed through Fisher's criterion by (7):

$$\boldsymbol{W} = \arg\max \frac{|W^T S_b W|}{|W^T S_w W|} \tag{7}$$

Therefore, the dimensionality reduction and/or feature space transformation is carried out by projecting the original feature matrix $\mathbf{T} \in \mathbb{R}^T$ $\boldsymbol{W}$ by (8):

$$\boldsymbol{V} = \boldsymbol{W}^T \boldsymbol{T} \tag{8}$$

where, $\boldsymbol{V}$ is a new set of extracted features that represent the original feature space into a lower dimension, i,e, 2-*D* or 3-*D* space where the evaluated conditions are visually represented (healthy, 25%, 50% and 75% of wear).

Then, in the fifth step of fault diagnosis, the features extracted by the LDA technique are then subjected to an automatic fault decision process using a Neural Network (NN)-based classifier. The NN-based classifier is achieved by a classical structure that only considers the input layer, a single hidden layer, and the output layer. This classical structure is implemented since the feature reduction procedure allows to facilitate the classification task. The representation of the implemented NN-based classifier is shown in Fig. 2, as it is observed, the proposed classifier consists of three layers where the input layer has ade fined number of neurons equal to features extracted by the LDA, the hidden layer considers ten neurons as suggested by the literature and the output layer comprises four neurons associated to the assesses conditions.

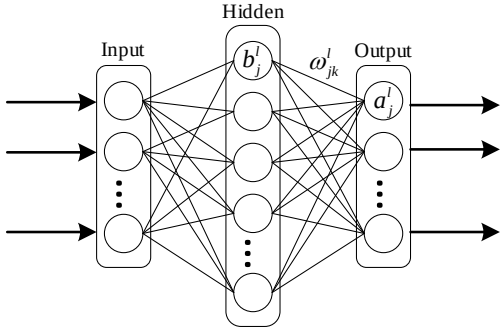

Fig. 2. Basic structure of a NN-based classifier.

Where, ω_{jk}^l is the weight from the *k*-th neuron in the $(l-1)$th layer to the *j*-th neuron in the *l*-th layer, and the activation of the a_j^l of the *j*th neuron in the *l*-th layer is associated with the activation in the $(l-1)$th layer by (9):

$$a_j^l = \sum_k \omega_{jk}^l a_k^{l-1} + b_j^l \tag{9}$$

IV. Experimental Test Bench

The proposed method is evaluated with a set of experimental data that were collected in a laboratory test bench. Such test bench is based on a kinematic chain that comprises an induction motor (IM) with 2P, 1 hp, 220 V (WEG 00236ET3E145T-W22), a gearbox with ratio 4:1 (BALDOR GCF4X01AA) and an automotive alternator that is used as a load. The IM speed is controlled by a variable frequency drive (VFD); the startup is set to a linear profile based on the variation of the supply frequency from 0 Hz to 60 Hz in 5 seconds. The four considered fault conditions (healthy condition and three different levels of uniform wear on the gear teeth) are successively tested using the specified 4:1 ratio gearbox. The automotive alternator acting as mechanical load was setup so that the IM operates at 10% of its rated load, for the results shown in this paper. The whole laboratory kinematic chain is shown in Fig. 3.

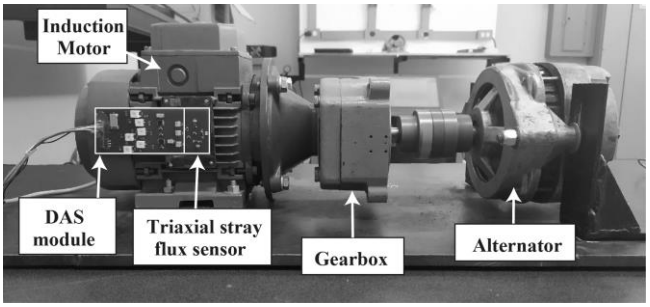

Fig. 3. Laboratory test bench based on a kinematic chain for the experimental evaluation of different levels of wear on the gear teeth in a gearbox.

The stray flux magnetic signals of the IM are acquired through three different hall-effect stray flux transducers that are perpendicularly installed between them allowing the measurement in the radial, axial and radial+axial axes, as it is proposed in [23]. These sensors allow an easy installation since are mounted on a board with its corresponding signal conditioning. Thus the magnetic flux signals of the IM are affected depending on whether the IM is operating under the influence of mechanical or electrical faults; in this sense, the sensors are located on one of the sides of the IM at a single point of the motor frame, in the plate, where the electrical and mechanical specifications of the IM are given. The signals are acquired through a proprietary data acquisition system (DAS) module (having a14-bit analog-to-digital converter) with a sampling rate of 5 kHz during a 30 seconds: the first 5 seconds correspond to the startup transient, while the remaining 25 seconds correspond to the steady-state.

The considered fault condition relies on a uniform wear in the gear that is an incipient fault which has received little attention in previous literature of the area. In this way, four conditions are considered: healthy gear and gear with three different levels of uniform wear on the teeth (25%, 50% and 75%); each one of these four conditions may be observed in Fig. 4 (a) to Fig. 4 (d), respectively. The uniform teeth wear levels were artificially induced during the manufacturing of the gears.

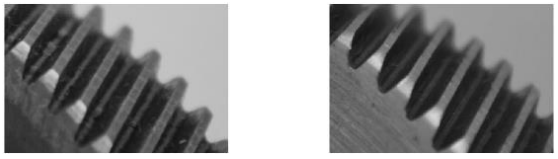

(a)

(b)

(c)

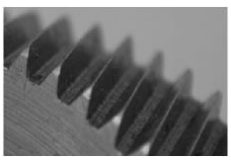

(d)

Fig. 4. Set of analysed gears: (a) healthy gear, and uniform wear on the gear teeth (b) 25%, (c) 50% and (d) 75%, respectively.

V. Results and Validation

A. Evaluation of the proposed method

The results provided in this section are obtained by applying the proposed diagnosis methodology to assess the gearbox condition. Thus, as commented above, the considered conditions are experimentally tested in the kinematic chain by replacing the healthy gear with each of the worn gears. Subsequently, for each evaluated condition, the stray flux signals are continuously acquired during the IM working condition while it is driven through the VFD, with 60 Hz as a supply frequency. Each one of the experiments was carried out several times to acquire different signals that allow to verify the repeatability of the results; as a result, there are at least 175 seconds of acquired data for each evaluated condition.

Afterwards, each acquired signal is characterized by means of estimating a meaningful set of 15 statistical time domain-based features, as a result, it is obtained a characteristic feature matrix with $TD = 45$ statistical features is computed, $\mathbf{T} \in \mathbb{R}^{TD}$. Also, previous to feature estimation, the acquired signals are subjected to a segmentation procedure by dividing the acquired signals in equal parts of 1 second. The segmentation procedure is performed to obtain a consecutive set of samples. Therefore, by considering each $\mathbf{q}_i$ as each stray flux available signal, for j=1,2,…,P, the segmentation procedure is achieved by following (10):

$$\mathbf{q}_i = \left[\mathbf{q}_i^{1:K}, \mathbf{q}_i^{L+1:2K}, \dots, \mathbf{q}_i^{(((n/K)-1)n)+1:n}\right] \qquad (10)$$

where K is the length of the time windows (more precisely, it is the number of sampled points for each segmented part of the signal); n is the total number of sampled points for each available signal. Hence, each available stray flux signal is divided in equal parts obtaining n/K segments. As a result of the feature estimation process, it is obtained a characteristic feature matrix for each one of the studied conditions. That is, the resulting feature matrix has a representation into a 45-dimensional space with 175 consecutive samples. Accordingly, the addressed conditions (healthy, and 25%, 50% and 75% of uniform wear in the teeth gear) are represented by their characteristic feature matrices.

Subsequently, following the proposed diagnosis methodology, the estimated feature matrices are subjected to the feature reduction procedure by means of applying the PCA and LDA technique. To this end, such matrices are first subjected to the dimensionality reduction procedure through the PCA to analyze the distribution of the data for all evaluated conditions. Table I summarizes the achieved eigenvalues, individual variance and the cumulative variance for the first seven principal components (PCs); note that, if the first two PCs are selected to represent the original feature space, then, a representation into a 2-dimensional space by retaining a cumulative variance equal to 98.791% from the original feature space will be achieved. Although, the analyzed features have a specific physical representation, i.e. RMS value, kurtosis, skewness, among other, the resulting Eigenvalues are considered as dimensionless due to there are only considered for estimating both values of variance percentage.

In accordance, the estimated features matrices, for all addressed conditions, are subjected to the dimensionality reduction procedure by means of the LDA technique and the original 15-dimensional feature space is transformed and projected into a 2-dimensional space to obtain a visual representation of the assessed conditions. In this regard, it must be highlighted that the most representative and discriminative information is retained by the LDA, which pursues the maximization of the linear separation between studied conditions. The obtained 2-dimensional projection is shown in Fig. 5; note that the four considered conditions are clearly separated from each other. The separation between the evaluated conditions is due to the fact that the resulting projection belongs to the linear combination of different weights of the statistical features; those statistical features with higher weights are considered as the most discriminative, i.e., they contain the most significative information that leads to a linear separation between the analysed conditions.

Following the proposed diagnosis methodology, the last step relies on the automatic fault diagnosis through a classical NN-based classifier. Thereby, the considered NN-based classifier has three layers; the input layer consists of two neurons in which each neuron represents each of the features extracted by

TABLE I Resulting Eigenvalues, Individual and Cumulative Variance for the PCs

Number of PC	Eigenvalues	Individual variance (%)	Cumulative variance (%)
PC1	1911.1	94.542	94.542
PC2	85.891	4.248	98.791
PC3	21.184	1.047	99.839
PC4	2.024	0.100	99.939
PC5	0.064	0.056	99.9953
PC6	0.016	0.003	99.998
PC7	0.012	8.33×10^{-4}	>99.999

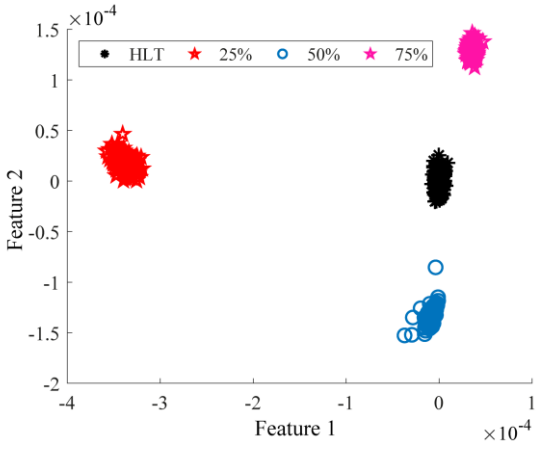

Fig. 5. Resulting 2-dimensional representation obtained by applying the LDA technique to the characteristic feature matrices for all

the LDA technique, i.e., Feature 1 and Feature 2. The hidden layer is a single layer based on ten neurons, as several state-of-the-art works recommend. Finally, the output layer is based on four neurons representing each one of the assessed conditions. Additionally, the NN-based classifier is trained and tested under a *k*-fold cross-validation scheme, with *k*=5, to obtain statistically significant results. Thus, the samples of the 2-dimensional set of extracted features are divided in two parts; the first one (with 140 samples per condition) is used during the training procedure and, the second one (with 35 samples per condition) is used during the test and validation. The proposed classifier is trained during 70 epochs and the backpropagation algorithm with the sigmoid function is used as the activation method. During the training and test, the proposed NN-based classifier reaches values of 99.8% and 100% as global classification ratios, respectively. Particularly, the individual results achieved for each one of the assessed conditions are summarized by the confusion matrix in Table II; note that only one misclassification error occurs during the training procedure whereas the test procedure fits all the samples to its corresponding class. These high-performance results prove that the consideration of the feature calculation and feature reduction stages leads to achieve a proper signal characterization of the evaluated conditions.

Moreover, the consideration of the proposed NN-based classifier also allows to obtain the decision regions that are modelled over the 2-dimensional projection where all addressed conditions are represented. In this sense, Fig. 6 shows the resulting decision regions that are modelled by the NN-based classifier for each considered condition during the training procedure. Even if one single sample of the condition related to 50% of uniform wear is misclassified, by means of the predicted percentage of membership function, it may be re-evaluated, and such misclassification error can be assigned to its corresponding true class.

B. Validation and comparison with ST-MUSIC

For validating the effectiveness of the proposed method, a comparative analysis is carried out by analyzing the time-frequency maps of the three stray flux acquired signals corresponding to the considered condition. In this regard, it is considered that the mechanical vibrations produced by gears are inherent to its operation due to the backlash or the excitation of the dynamic [1]. Thereby, the backlash leads to an increase of the vibration amplitude known as the mesh frequency (f_{mesh}), and mesh-related frequencies ($f_{Gr1mesh}$) which can be observed in the vibration and torque spectra; such components are described by (11) and (12), respectively [24]:

$$f_{mesh} = N_{r1} \cdot f_{r1} = N_{r2} \cdot f_{r2} \tag{11}$$

$$f_{Gr1mesh} = N_{r1} \cdot f_{r1} \pm f_{r1} \tag{12}$$

where N_{r1} and N_{r2} are the number of input and output gear teeth, respectively, and f_{r1} and f_{r2} are the input and output rotating frequency, respectively.

Moreover, in [25] it is shown that, in presence of gearbox faults, any torsional vibration in the rotor will introduce

TABLE II CONFUSION MATRIX ACHIEVED BY THE RESULTING INDIVIDUAL CLASSIFICATION THROUGH THE PROPOSED NN-BASED CLASSIFIER

		True class							
		Training				Test			
		HLT	25%	50%	75%	HLT	25%	50%	75%
Assigned class	HLT	140	0	1	0	35	0	0	0
	25%	0	140	0	0	0	35	0	0
	50%	0	0	139	0	0	0	35	0
	75%	0	0	0	140	0	0	0	35

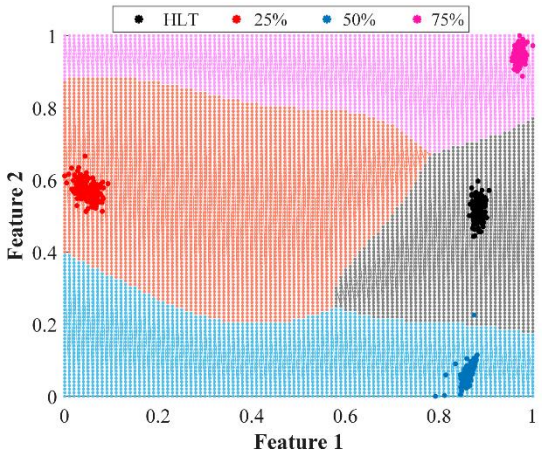

Fig. 6. Resulting decision regions modelled by the proposed NN-based classifier over the 2-dimensional space where all considered conditions are represented.

families of sidebands harmonics induced either by the rotation of the input gear (f_{Gr1}), the rotation of the output gear (f_{Gr2}), or the stiffness variation of the gear teeth contact (f_{Gmesh}). In addition, the combination of componenets associated with the input and output gears, f_{Gr1} and f_{Gr2}, can also appear producing the amplification its related harmonics ($f_{Gr1-Gr2}$). Moreover, the appearance of characteristic frequency compoenents associated to the input gear and mesh frequency ($f_{Gr1-mesh}$), and associated with the output gear and mesh frequency ($f_{Gr1-Gr2-mesh}$) are similarly generated. Such sidebands harmonics can be observed around the power supply frequency (f_s) of the stator current, and their location is given by (13) to (18).

$$f_{Gr1} = f_s \pm m \cdot f_{r1} \tag{13}$$

$$f_{Gr2} = f_s \pm n \cdot f_{r2} \tag{14}$$

$$f_{Gmesh} = f_s \pm p \cdot f_{mesh} \tag{15}$$

$$f_{Gr1-Gr2} = f_s \pm m \cdot f_{r1} \pm n \cdot f_{r2} \tag{16}$$

$$f_{Gr1-mesh} = f_s \pm m \cdot f_{r1} \pm p \cdot f_{mesh} \tag{17}$$

$$f_{Gr1-Gr2-mesh} = f_s \pm m \cdot f_{r1} \pm n \cdot f_{r2} \pm p \cdot f_{mesh} \tag{18}$$

where *m*, *n* and *p* represent a positive integer number that can take values equal to 1, 2, 3, …that allows computing the corresponding harmonics of the fundamental components f_{Gr1}, $f_{Gr2}$and f_{Gmesh}, respectively, in a frequency spectrum.

Likewise, as pointed out in [26], the stray flux of an electric motor is the magnetic flux that radiates outside the frame of the machine induced by stator and rotor currents. These currents (and hence the stray flux) are modified when the electric motor and/or an element linked to the electric motor operates under a fault condition [27]. Consequently, in the case of gearboxes driven by electric motors, the stray flux signals can suffer changes due to a gearbox fault; and, due to the fault harmonic components being slip-dependent, a fault-related pattern is expected in the stray flux signals during the start-up transient, as it happened with other faults [27].

Accordingly, the validation consists in the comparison and analysis of the results achieved in the previous reported work [19]; where, the short-time MUSIC (ST-MUSIC) algorithm is implemented in order to identify those fault-related frequency components described by (13) to (18). Indeed, through the ST-MUSIC it is performed the transient analysis of the three stray flux signals captured during the experimental evaluation of each studied condition.Hence, **¡Error! No se encuentra el origen de la referencia.**

TABLE III MAXIMUM AMPLITUDE TRACKED FOR f_{Gr2} FAULT-RELATED HARMONIC

Teeth gear condition	f_{Gr2} maximum amplitude tracked (dB)		
	Radial stray flux	*Axial stray flux*	*Axial + radial stray flux*
Healthy gear	-43.80	-49.890	-42.165
25 % of wear	-42.21	-46.450	-37.648
50 % of wear	-41.58	-48.60	-34.30
75 % of wear	-32.97	-47.300	-31.77

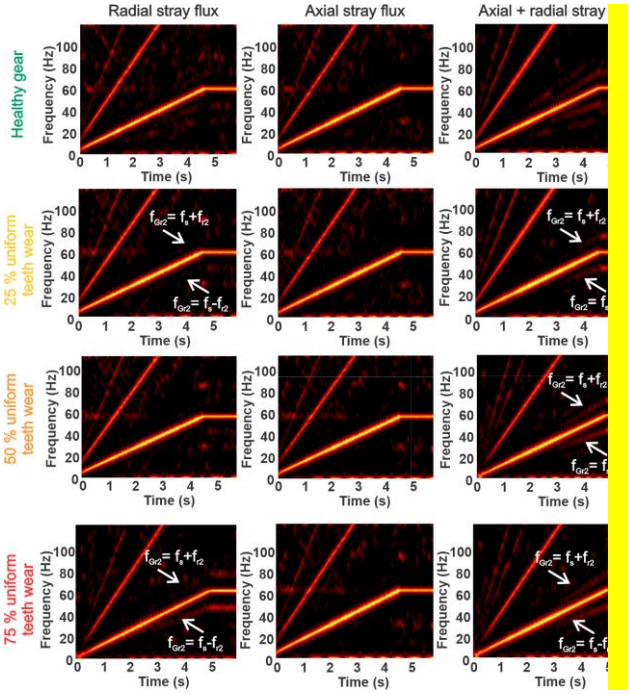

Fig. 7. MUSIC analyses of the stray flux signals under starting for the different fault conditions, healthy gear, and three fault conditions of uniform wear on the gear teeth 25%, 50% and 75%.

shows the resulting time–frequency (t-f) maps where it is possible to observe the characteristic fault-related time-frequency patterns that are caused by the amplified fault components predicted in the theory. Particularly, when analyzing the t-f map that corresponds to the axial + radial stray flux signal, it is clearly visible the evolution during the start-up transient of the fault frequency component $f_{Gr2} = f_s \pm n \cdot f_{r2}$ with $n = 1$, for the cases when the kinematic chain is working the uniform wear conditions (i.e., 25%, 50% and 75% of uniform wear in the teeth gear).s

On the contrary, when the gearbox is in a healthy state, the characteristic fault-related component does not appear. Moreover, **¡Error! No se encuentra el origen de la referencia.** shows that there is not a specific pattern related to a fault component in the axial stray flux while the radial stray flux shows a certain amplitude f_{Gr2} fault evolution. Additionally, Table III shows the maximum amplitude achieved for the f_{GR2} fault-related harmonic and for the different studied cases. Note that the f_{GR2} frequency component obtained by analysing the radial stray flux shows an amplitude of -43.80 dB for a healthy gear; in contrast, the same frequency component for a 75 % uniform teeth wear has a maximum achieved amplitude of -32.97 dB. Similarly, by analysing the axial + radial stray flux it is obtained a f_{GR2} maximum amplitude of -42.165 dB for a healthy gear, -37.648 dB for a 25% of uniform wear, -34.30 dB for a 50% of uniform wear and -31.77 dB for a 75 % of uniform wear in the teeth gear. This situation allows to discriminate between an incipient wear in the gear and a healthy gear by comparing the maximum amplitude of the f_{GR2} fault-related harmonic during the start-up. Additionally, this condition shows that gearbox faults mainly affect the radial flux. On the other hand, the maximum amplitude tracked for the axial stray flux shows a minimum difference among the different studied wear conditions. Although through the analysis of the t-f maps it is possible to identify the occurrence of gearbox faults, such as uniform wear in the teeth gear, the condition assessment is limited to be performed as a manual procedure, in which the characteristic fault-related frequency components must be identified and compared, a fact that justifies the value of the method proposed in this work.

TABLE III MAXIMUM AMPLITUDE TRACKED FOR f_{Gr2} FAULT-RELATED HARMONIC

Teeth gear condition	f_{Gr2} maximum amplitude tracked (dB)		
	Radial stray flux	*Axial stray flux*	*Axial + radial stray flux*
Healthy gear	-43.80	-49.890	-42.165
25 % of wear	-42.21	-46.450	-37.648
50 % of wear	-41.58	-48.60	-34.30
75 % of wear	-32.97	-47.300	-31.77

VI. CONCLUSIONS

In this paper, a novel condition monitoring approach for the condition assessment of a gearbox under the incipient fault conditions of uniform wear in the teeth is proposed. The method

is based on the analysis of stray flux signals that are captured during the operation of an induction motor that drives the gearbox under observation. There are three important aspects of the proposed approach that must be highlighted; first, the condition assessment proposal that leads to the identification of an incipient fault such as the uniform wear in the teeth gear which shows superiority in comparison with other related works in which discrete faults have been analysed, i.e., chipped or fully broken teeth in a gear. Second, the analysis of stray flux signals and its characterization through the estimation of a meaningful set of statistical time domain-based features that leads to a high-performance feature pattern characterization of the different evaluated conditions. Third, the analysis of the estimated set of features through PCA, which facilities to determine the minimum number of dimensions that are required to represent the original feature space with any information loss, also, the use of the LDA technique to obtain a 2-dimensional representation where all considered conditions are clearly separated between them. Finally, the feature reduction through the LDA facilitates the classification task for the proposed classical structure of the NN-based classifier; indeed, the global classification ratio achieved by the NN-based classifier is higher than 99.8%. Moreover, regarding the comparison with ST-MUSIC, it should be mentioned that the proposed method has also advantages since it yields an automatic fault diagnosis and classification, whereas the simple use of the ST-MUSIC method requires additional user expertise to identify the fault-related components in the resulting time-frequency maps, a fact that suggests the use of ST-MUSIC for offline analysis, being and less suitable to automatic condition monitoring systems. The high-performance results demonstrate the effectiveness of the proposed and make the proposed method suitable to be implemented as a non-invasive diagnostic tool that may be incorporated in the Condition-Based Maintenance programs for industrial applications.

REFERENCES

[1] J. J. Saucedo-Dorantes, M. Delgado-Prieto, J. A. Ortega-Redondo, R. A. Osornio-Rios, and R. D. J. Romero-Troncoso, “Multiple-Fault Detection Methodology Based on Vibration and Current Analysis Applied to Bearings in Induction Motors and Gearboxes on the Kinematic Chain,” Shock Vib., vol. 2016, 2016, doi: 10.1155/2016/5467643.

[2] J. P. Salameh, S. Cauet, E. Etien, A. Sakout, and L. Rambault, “Gearbox condition monitoring in wind turbines: A review,” Mech. Syst. Signal Process., vol. 111, pp. 251–264, 2018, doi: 10.1016/j.ymssp.2018.03.052.

[3] T. Praveenkumar, M. Saimurugan, and K. I. Ramachandran, “Comparison of vibration, sound and motor current signature analysis for detection of gear box faults,” Int. J. Progn. Heal. Manag., vol. 8, no. 2, pp. 1–10, 2017, doi: 10.36001/ijphm.2017.v8i2.2642.

[4] M. Azamfar, J. Singh, I. Bravo-Imaz, and J. Lee, “Multisensor data fusion for gearbox fault diagnosis using 2-D convolutional neural network and motor current signature analysis,” Mech. Syst. Signal Process., vol. 144, p. 106861, 2020, doi: 10.1016/j.ymssp.2020.106861.

[5] X. Jin, F. Cheng, Y. Peng, W. Qiao and L. Qu, "Drivetrain Gearbox Fault Diagnosis: Vibration- and Current-Based Approaches," in IEEE Industry Applications Magazine, vol. 24, no. 6, pp. 56-66, Nov.-Dec. 2018, doi: 10.1109/MIAS.2017.2740470.

[6] S. H. Kia, H. Henao, and G. A. Capolino, “Analytical and experimental study of gearbox mechanical effect on the induction machine stator current signature,” IEEE Trans. Ind. Appl., vol. 45, no. 4, pp. 1405–1415, 2009, doi: 10.1109/TIA.2009.2023503.

[7] R. Zhang, F. Gu, H. Mansaf, T. Wang, and A. D. Ball, “Gear wear monitoring by modulation signal bispectrum based on motor current signal analysis,” Mech. Syst. Signal Process., vol. 94, pp. 202–213, 2017, doi: 10.1016/j.ymssp.2017.02.037.

[8] I. Bravo-Imaz, H. Davari Ardakani, Z. Liu, A. García-Arribas, A. Arnaiz, and J. Lee, “Motor current signature analysis for gearbox condition monitoring under transient speeds using wavelet analysis and dual-level time synchronous averaging,” Mech. Syst. Signal Process., vol. 94, pp. 73–84, 2017, doi: 10.1016/j.ymssp.2017.02.011.

[9] M. H. Marzebali, J. Faiz, G. Capolino, S. H. Kia and H. Henao, "Planetary Gear Fault Detection Based on Mechanical Torque and Stator Current Signatures of a Wound Rotor Induction Generator," in IEEE Transactions on Energy Conversion, vol. 33, no. 3, pp. 1072-1085, Sept. 2018, doi: 10.1109/TEC.2018.2811044.

[10] A. Parey and A. Singh, “Gearbox fault diagnosis using acoustic signals, continuous wavelet transform and adaptive neuro-fuzzy inference system,” Applied Acoustics, vol. 147, pp. 133-140, 2019.

[11] S. M. J. Rastegar Fatemi, H. Henao, and G. A. Capolino, “Gearbox monitoring by using the stray flux in an induction machine based electromechanical system,” in Proceedings of the Mediterranean Electrotechnical Conference - MELECON, 2008, pp. 484–489, doi: 10.1109/MELCON.2008.4618482.

[12] S. M. J. R. Fatemi, H. Henao, and G. A. Capolino, “The effect of the mechanical behavior on the stray flux in an induction machine based electromechanical system,” 2007 IEEE Int. Symp. Diagnostics Electr. Mach. Power Electron. Drives, SDEMPED, pp. 155–160, 2007, doi: 10.1109/DEMPED.2007.4393087.

[13] Y. Park, H. Choi, J. Shin, J. Park, S. Bin Lee, and H. Jo, “Airgap flux based detection and classification of induction motor rotor and load defects during the starting transient,” IEEE Trans. Ind. Electron., vol. 67, no. 12, pp. 10075–10084, 2020, doi: 10.1109/TIE.2019.2962470.

[14] K. N. Gyftakis, P. A. Panagiotou, and D. Spyrakis, “Recent Experiences with MCSA and Flux Condition Monitoring of Mechanical Faults in 6kV Induction Motors for Water Pumping Applications,” in Proceedings of the 2019 IEEE 12th International Symposium on Diagnostics for Electrical Machines, Power Electronics and Drives, SDEMPED 2019, 2019, pp. 214–219, doi: 10.1109/DEMPED.2019.8864923.

[15] S.-B. Lee, J. Shin, Y. Park, H. Kim, and J. Kim, “Reliable Flux based Detection of Induction Motor Rotor Faults from the 5th Rotor Rotational Frequency Sideband,” IEEE Trans. Ind. Electron., vol. 0046, no. c, pp. 1–1, 2020, doi: 10.1109/tie.2020.3016241.

[16] Y. Park, C. Yang, J. Kim, H. Kim, S. B. Lee, K. N. Gyftakis, P. A. Panagiotou, S. H. Kia and G. A. Capolino, “Stray flux monitoring for reliable detection of rotor faults under the influence of rotor axial air ducts,” IEEE Trans. Ind. Electron., vol. 66, no. 10, pp. 7561–7570, 2019, doi: 10.1109/TIE.2018.2880670.

[17] J. J. Saucedo-Dorantes, M. Delgado-Prieto, R. A. Osornio-Rios and R. de Jesus Romero-Troncoso, "Multifault Diagnosis Method Applied to an Electric Machine Based on High-Dimensional Feature Reduction," in IEEE Transactions on Industry Applications, vol. 53, no. 3, pp. 3086-3097, May-June 2017, doi: 10.1109/TIA.2016.2637307.

[18] H. O. A. Ahmed and A. K. Nandi, "Three-Stage Hybrid Fault Diagnosis for Rolling Bearings With Compressively Sampled Data and Subspace Learning Techniques," in IEEE Transactions on Industrial Electronics, vol. 66, no. 7, pp. 5516-5524, July 2019, doi: 10.1109/TIE.2018.2868259.

[19] I. Zamudio-Ramírez, J. A. Antonino-Daviu and R. A. Osornio-Ríos, “Transient Stray Flux Analysis Via MUSIC Methods for the Detection of Uniform Gearbox Teeth Wear Faults,” *In proceedings of the 13th Annual IEEE Energy Conversion Congress & Exposition (ECCE 2021),* Vancouver, Canada, 2021.

[20] T. Wang, Q. Han, F. Chu and Z. Feng, “Vibration based condition monitoring and fault diagnosis of wind turbine planetary gearbox: A review,” Mechanical Systems and Signal Processing, vol. 126, pp. 662-685, 2019.

[21] R. O. Duda, P. E. Hart and D. G. Stork, Pattern Classification, 2nd Edition, Wiley-Interscience, 2000.

[22] S. Zolfaghari, S. B. M Noor, M. R. Mehrjou,M. H. Marhaban and N. Mariun, “Broken Rotor Bar Fault Detection and Classification Using Wavelet Packet Signature Analysis Based on Fourier Transform and Multi-Layer Perceptron Neural Network,” Applied Sciences, vol. 8, no. 1, 2018, doi.org/10.3390/app8010025.

[23] I. Zamudio-Ramírez, R. A. Osornio-Ríos, J. A. Antonino-Daviu, and A. Quijano-Lopez, “Smart-sensor for the automatic detection of electromechanical faults in induction motors based on the transient stray flux analysis,” Sensors (Switzerland), vol. 20, no. 5, 2020, doi: 10.3390/s20051477.

[24] J. H. Kuang and A. D. Lin, "Theoretical aspects of torque responses in spur gearing due to mesh stiffness variation," Mech. Syst. Signal Process., vol. 17, no. 2, pp. 255–271, 2003, doi: 10.1006/mssp.2002.1516.
[25] S. H. Kia, H. Hénao, and G. A. Capolino, "Gearbox monitoring using induction machine stator current analysis," 2007 IEEE Int. Symp. Diagnostics Electr. Mach. Power Electron. Drives, SDEMPED, pp. 149–154, 2007, doi: 10.1109/DEMPED.2007.4393086.
[26] R. Romary, R. Pusca, J. P. Lecointe, and J. F. Brudny, "Electrical machines fault diagnosis by stray flux analysis," in Proceedings - 2013 IEEE Workshop on Electrical Machines Design, Control and Diagnosis, WEMDCD 2013, 2013, pp. 247–256, doi: 10.1109/WEMDCD.2013.6525184.
[27] J. A. Ramirez-Nunez, J. A. Antonino-Daviu, V. Climente-Alarcon, A. Quijano-Lopez, H. Razink and R. A. Osornio-Rios., "Evaluation of the Detectability of Electromechanical Faults in Induction Motors Via Transient Analysis of the Stray Flux," IEEE Trans. Ind. Appl., vol. 54, no. 5, pp. 4324–4332, 2018, doi: 10.1109/TIA.2018.2843371.

Israel Zamudio-Ramírez (Fellow, IEEE). Israel Zamudio-Ramírez received the M.S. degree in mechatronic from the Autonomous University of Queretaro, Mexico, in 2019. He is currently working toward the Ph.D. degree in mechatronics at the Autonomous University of Queretaro with the Department of Mechatronics, Mexico and in electrical engineering at the Universitat Politècnica de València with the Department of Electrical Engineering, Spain. His research interests include monitoring and diagnosis of electrical machines, embedded systems and hardware signal processing for engineering applications on FPGA.

Juan Jose Saucedo-Dorantes (Member, IEEE), received the M. E. and Ph. D degrees in mechatronics from the Autonomous University of Queretaro (UAQ), Queretaro, Mexico, in 2014 and 2018, respectively. Since 2012, he has been doing research work at the HSPdigital research group. He is a National Researcher level 1 with the Mexican Council of Science and Technology, CONACYT, and is currently a Head Professor with the UAQ, Queretaro, Mexico. His research interests include digital signal processing on FPGAs for applications in engineering, condition monitoring and fault diagnosis in electromechanical systems, fault detection algorithms, artificial intelligence and signal processing methods.

Jose Antonino-Daviu (S'04, M'08, SM'12) received his M.S. and Ph. D. degrees in Electrical Engineering, both from the Universitat Politècnica de València, in 2000 and 2006, respectively. He also received his Bs. in Business Administration from Universitat de Valencia in 2012. He was working for IBM during 2 years, being involved in several international projects. Currently, he is Full Professor in the Department of Electrical Engineering of the mentioned University, where he develops his docent and research work. He has been invited professor in Helsinki University of Technology (Finland) in 2005 and 2007, Michigan State University (USA) in 2010, Korea University (Korea) in 2014 and Université Claude Bernard Lyon 1 (France) in 2015. He is IEEE Senior Member since 2012 and he has published over 200 contributions, including international journals, conferences and books. He is also Associate Editor of IEEE transactions on Industrial Informatics and IEEE Industrial Electronics Magazine and he is also IEEE IAS Distinguished Lecturer for 2019-20. He was General Co-Chair of IEEE SDEMPED 2013. He received the Nagamori Award from Nagamori Fundation in Kyoto, Japan in 2018, for his contributions in electric motors transient analysis area. In 2019, he was awarded with the SDEMPED Diagnostic Achievement Award in Toulouse, France.

Roque Alfredo Osornio-Rios (M'11, SM'21), received the Ph.D. degree in mechatronics from the Autonomous University of Queretaro, Queretaro, Mexico, in 2007. He is a National Researcher level 3 with the Mexican Council of Science and Technology, CONACYT. He is currently a Head Professor with the Department of Mechatronics, University of Queretaro. He is an Advisor for more than 80 theses, and has coauthored more than 100 technical papers published in international journals and conferences. His research interests include hardware signal processing and mechatronics. Dr. Osornio-Rios is a Fellow of the Mexican Academy of Engineering. He is part of the editorial board of Journal and Scientific and Industrial Research and member of the IEEE IES Electrical Machines Technical Committee.

Larisa Dunai (M´19), Associate Professor at Universitat Politecnica de Valencia (UPV), obtained her MSc degree in Electronic Engineering in 2003 from Technical University of Moldova. Afterwards, she joined that University as an Assistant professor at the Radio electronics and Telecommunications Department. In 2007 she started working as a researcher in the Research Center in Graphic Technology (CITG) of the UPV. In November 2008 she became Assistant professor of the Graphic Design Department. In 2010 obtained her PhD at UPV. In 2013 she received the MIT Innovators Award for Spain and in 2014 the Michael Richey Medal from Royal Institute of Navigation (UK).